Pyrolysis Chemistry of Sol−Gel-Derived Poly(dimethylsiloxane)−Zirconia Nanocomposites. Influence of Zirconium on Polymer-to-Ceramic Conversion

Sandra Dirè,* Renzo Campostrini, and Riccardo Ceccato

Dipartimento di Ingegneria dei Materiali, Università di Trento, via Mesiano 77, 38050 Trento, Italy

Received June 11, 1997. Revised Manuscript Received September 30, 1997[⊗]

The pyrolytic transformation of hybrid gels, obtained by hydrolysis−condensation of diethoxydimethylsilane and zirconium *n*-propoxide mixtures with different Si/Zr ratio, has been studied using TG−GC−MS coupled techniques, FTIR spectroscopy, and N_2 adsorption analysis. The starting gels have been described as nanocomposites formed with poly(dimethylsiloxane) chains and oxide particles. The pyrolysis pathway appears to be strongly dependent on the chemical composition of the xerogels. The evolution of methane is observed throughout the whole thermal process and increases with increasing zirconia content. The presence of zirconium atoms causes a decrease in thermal stability of the Si−C bonds in the $SiMe_2O$ units with the evolution of methane starting at temperature as low as 275 °C. For zirconium percentages up to 30%, the thermal treatment leads mainly to the loss of cyclic oligomers either entrapped in the siloxane matrix during the gelling process or released through rearrangement reactions based on Si−O/Si−O and Si−C/Si−O bond exchanges along the poly(dimethylsiloxane) chains. A different pyrolytic behavior is observed for the sample containing 50% ZrO_2 which exhibits the release of siloxane dimers and tetramethylsilane. From the pyrolysis pathways, different structural arrangements between zirconia particles and the organic-modified counterpart are proposed as a function of chemical composition.

Introduction

A common route to modify the sol−gel-derived oxide networks is the use of organosilanes containing Si−C bonds which are stable toward the hydrolysis−condensation reactions.[1] Usually, the inorganic counterpart is built up by gelation of tetrafunctional silicon alkoxide solutions.[2−4] More recently, a new family of hybrid organic−inorganic materials has been obtained by reacting the difunctional diethoxydimethylsilane (DEDMS), which has the role of a network modifier, with transition metal alkoxides (TMA) acting as network formers.[5,6] The solution and low-temperature solid state chemistry of DEDMS/TMA-derived gels has been extensively studied by liquid and solid-state NMR, which have demonstrated the activity of titanium and zirconium alkoxides in promoting the condensation of the difunctional silicon precursor through the formation of intermediates containing Si−O−M (M = Zr, Ti) bonds, finally yielding siloxane polymers.[6−8] The structural characterization of the oxide moiety by X-ray absorption techniques reveals, in the case of DEDMS/$Ti(OPr^i)_4$ xerogels, that oxide particles produced in the network should be in the nanometer size range, according to the transparency of the samples.[9,10] A definite description of the DEDMS/TMA-derived gels has been given in terms of nanocomposites made of long chains cross-linked by oxide particles.[5,6,10]

Hybrid gels are very attractive precursors for incorporating carbon into a silica network, yielding oxycarbide glasses or resulting in carbide composites.[11−16] Glasses and ceramics, obtained by firing organic-modified gels under a reducing atmosphere, are of interest for their chemical and mechanical properties.[17] These features are expected to improve with the presence of a transition metal.

[⊗] Abstract published in *Advance ACS Abstracts,* November 15, 1997.

(1) Schmidt, H.; Seiferling, B. *Mat. Res. Soc. Symp. Proc.* **1986**, *73*, 739.
(2) Schmidt, H. *Mater. Res. Soc. Symp. Proc.* **1990**, *180*, 961.
(3) Babonneau, F.; Bois, L.; Maquet, J.; Livage, J. in *Eurogel '91*; Vilminot, S., Nass, R., Schmidt, H., Eds.; Elsevier Science Publ.: Amsterdam, The Netherlands 1992, p 319.
(4) Glaser, R. H.; Wilkes, G. L.; Bronnimann, C. E. *J. Non-Cryst. Solids* **1989**, *113*, 73.
(5) Dirè, S.; Babonneau, F.; Sanchez, C.; Livage, J. *J. Mater. Chem.* **1992**, *2*, 239.
(6) Dirè, S.; Babonneau, F.; Carturan, G.; Livage, J. *J. Non-Cryst. Solids* **1992**, *147 & 148*, 62.
(7) Babonneau, F.; Maquet, J.; Dirè, S. J. *Polym. Prepr.* **1993**, *34*, 242.
(8) Babonneau, F. *Mater. Res. Soc. Symp. Proc.* **1994**, *346*, 949.
(9) Dirè, S.; Bois, L.; Babonneau, F.; Carturan, G. *Polym. Prepr.* **1991**, *32*, 501.
(10) Babonneau, F.; Bois, L.; Livage, J.; Dirè, S. *Mater. Res. Soc. Symp. Proc.* **1993**, *286*, 289.
(11) Babonneau, F.; Bois, L.; Livage, J. *J. Non-Cryst. Solids* **1992**, *147 & 148*, 280.
(12) Babonneau, F.; Thorne, K.; Mackenzie, J. D. *Chem. Mater.* **1989**, *1*, 554.
(13) Babonneau, F.; Sorarù, G. D.; D'Andrea, G.; Dirè, S.; Bois, L. *Mater. Res. Soc. Symp. Proc.* **1992**, *271*, 789.
(14) Burns, G. T.; Taylor, R. B.; Xu, Y.; Zangvil, A.; Zank, G. A. *Chem. Mater.* **1992**, *4*, 1313.
(15) Bois, L.; Maquet, J.; Babonneau, F.; Mutin, H.; Bahloul, D. *Chem. Mater.* **1994**, *6*, 796.
(16) Zhang, H.; Pantano, C. G. *J. Am. Ceram. Soc.* **1990**, *73*, 958.

S0897-4756(97)00414-6 CCC: $15.00
Published on Web 01/19/1998

In a previous study, we reported the production at high temperature of crystalline silica and titanium carbide composites by pyrolysis of a 70 DEDMS/30 Ti(OPr^i)$_4$ (mol %) xerogel (DTi30).[18] Using ^{29}Si MAS NMR, X-ray diffraction, and Ti K-edge X-ray absorption techniques, we found that the gel thermal stability was poor and that Si−C bond cleavage began at mild temperatures, leading to redistribution reactions around the silicon atom and the progressive coordination change of the titanium-based phase, with the Ti−O bonds, present at low temperature, replaced by Ti−C bonds starting from 800 °C. Though the structural evolution during pyrolysis was well-documented, no information was achieved about the mechanism of the polymer-to-ceramic conversion. Moreover, some differences between the behavior of titanium and zirconium as network formers in siloxane−oxide hybrids have been previously evidenced;[10] in particular, their ability to form heterometallic Si−O−M bonds and their stability in solution and in the solid state seem to be different for the two metals.[8,10]

The objective of the present work is to better understand the chemistry involved in the pyrolysis process of siloxane gels containing a zirconium oxide phase. Since this pyrolytic transformation is a very complicated process involving several reactions with the evolution of various gases, the firing of DEDMS/Zr(OPr^n)$_4$ xerogels is followed here by thermogravimetric analysis coupled with gas chromatographic and mass spectrometric analyses (TG−GC−MS).[19] FTIR and nitrogen adsorption results are also presented to propose a mechanism of ceramization and specify the role of the transition metal in the thermal conversion of the gel.

Experimental Section

Reagent grade diethoxydimethylsilane (DEDMS) and zirconium *n*-propoxide (ZR) were purchased from Fluka. Reagents used as standard for GC−MS analysis, hexamethyldisiloxane (M2), hexamethylcyclotrisiloxane (Cy3), octamethylcyclotetrasiloxane (Cy4), chlorotrimethylsilane (Si−Cl), and tetramethylsilane (TMS), were obtained by ABCR, whereas ethanol, *n*-propanol, propene, methane, and ethene were Carlo Erba RPE reagents. Reagents were used without further purification.

Synthesis of DZR*x* Gels. As previously reported,[5,7,10] a mixture of DEDMS, water, and ethanol in a 1:1:1 molar ratio was allowed to react for 3 min before addition of various amounts of ZR in order to obtain a Si:Zr molar ratio varying from 90:10 to 50:50. Reactions were performed in air at 25 °C. Samples were labeled DZR*x*, where D stands for the silicon precursor, ZR for zirconium alkoxide, and *x* is the molar percentage of ZR. The pH of the water was previously adjusted to 1 by addition of hydrochloric acid. The homogeneous sols were stirred for 15 min before casting in open vessels. Transparent and homogeneous gels with a light yellow coloration were obtained after a few days and aged at room temperature for several months. Monolithic and compliant xerogels were obtained up to 30% ZR, whereas DZR50 was brittle and powdered.

Samples were pyrolyzed at different temperatures up to 1400 °C with 1 °C min^{-1} heating rate in Ar flow in order to obtain samples for FTIR and surface area measurements. Samples pyrolyzed at 200 °C maintained the xerogel features, whereas further heating, above 600 °C, generated almost black samples.

Characterization Techniques. Thermogravimetric analyses (TG, DTG) were performed using a STA 409 Netzsch thermobalance and carried out under helium flow (100 mL min^{-1}) up to 1400 °C with 10 °C min^{-1} heating rate. Typically,100 mg of powdered samples were analyzed using α-allumina as reference.

Gas chromatographic analyses were obtained on a HRGC-Carlo Erba gas chromatograph employing a MEGA OV1 capillary column (25 m × 0.32 mm). The carrier gas was He at 20 kPa pressure, the selected temperature program was as follows: 30 °C for 5 min; first heating rate, 5 °C min^{-1} up to 100 °C, held for 1 min; second heating rate, 10 °C min^{-1} up to 200 °C, held for 20 min. Gas sampling was performed with a Bimatic thermostated microsample valve supplied with a 100 μL loop.

Mass spectrometric analyses were recorded with a VG QMD 1000 quadrupole mass spectrometer. Electron impact (70 eV) mass spectra were recorded with 1 s frequency, scanning from 2 to 300 amu.

The pyrolysis characterization was obtained with two experimental setups.[19,20] A first study was performed by directly analyzing the gases evolved during the TG experiments with the mass spectrometer (TG−MS) using a thermostated empty capillary column as transfer line. Results are presented as (a) the plot of TIC, total ion current (arising from the contribution of whole ionic fragments of each mass spectrum), vs time or pyrolysis temperature, drawn in order to analyze the presence of any evolving species, and (b) the contribution of an appropriate *m*/*z* ion current (IC) vs time, employed to monitor the evolution of a particular species during pyrolysis. For a more accurate determination of the evolved gases at various temperatures, gas fractions were gas chromatographically eluted before mass spectrometric detection (TG−GC−MS). The chemical species were determined on the basis of their mass spectra and retention times (t_R); these results were confirmed analyzing, under the same experimental conditions, pure reagents used as standards. The t_R values are calculated with respect to the first chromatographic peak generated by the contemporary elution of air, CH_4, CO_2, and CO. With the aim to compare the different amounts of species evolved during pyrolysis, a semiquantitative analysis was performed assuming that (1) the normalized chromatographic peak area is equal to the concentration of the eluted species and (2) for the species simultaneously eluted in the first chromatographic peak, the normalized intensity of a representative fragment ion in the mass spectrum accounts for its concentration.

FTIR spectra were recorded on a 5DXC Nicolet spectrophotometer in transmission mode using KBr pellets. A total of 64 scans were accumulated for each sample in the 4000−400 cm^{-1} interval, with 2 cm^{-1} resolution.

N_2 adsorption experiments at 77 K were performed on a Sorptomatic 1800 Carlo Erba instrument. 350 mg samples were degassed overnight at 80 °C before analysis. The BET equation was used for surface area calculation; it was linear in the interval $0.05 \leq p/p_0 \leq 0.33$ with a least-squares fit ≥ 0.998.

In this paper, we refer to the silicon units using the well-known NMR nomenclature: Q, T, D, and M units correspond to silicon atoms bonded to 4, 3, 2, and 1 oxygen atoms, respectively.

Results

Pyrolysis Characterization. From the comprehensive evaluation of the pyrolysis results, we present the characterization data starting from DZR30 xerogel which appears representative of the samples with lower

(17) Sorarù, G. D.; Sglavo, V. M.; Dirè, S.; D'Andrea, G.; Babonneau, F. in *3rd Euroceramics*, Duran, P., Fernandez, J. P., Eds.; Faenza Ed. Iberica: Castellón de le Plana, Spain, 1993, Vol. 2, p 1157.

(18) Dirè, S.; Babonneau, F. *J. Sol-Gel Sci. Technol.* **1994**, *2*, 139.

(19) Campostrini, R.; D'Andrea, G.; Carturan, G.; Ceccato, R.; Sorarù, G. D. *J. Mater. Chem.* **1996**, *6*, 585.

(20) Sorarù, G. D.; Campostrini, R.; D'Andrea, G.; Maurina, S. *Mater. Res. Soc. Symp. Proc.* **1996**, *435*, 381.

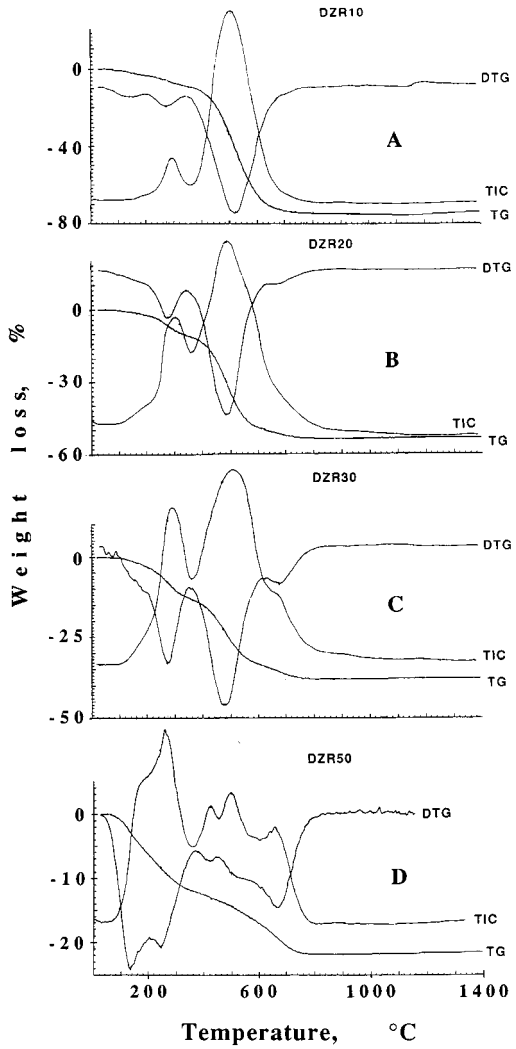

Figure 1. Comparison between TG, DTG, and TIC curves for DZR*x* gels: (A) $x = 10$, (B) $x = 20$, (C) $x = 30$, and (D) $x = 50$.

ZR content, whereas DZR50 pyrolysis shows a remarkable different trend and will be discussed later.

DZR30 Xerogel. Figure 1c shows the comparison of TG, DTG, and TIC curve for the DZR30 system. Three weight loss steps are found in the TG curve in the temperature intervals 60−360, 360−620, and 620−800 °C that correspond to 13.4, 20.8, and 3.9 wt % intensity, respectively. The DTG curve shows a peak at 272 °C and a more intense one at 470 °C together with shoulders at 160 and 675 °C. A similar trend is observed for the TIC curve with a slight increase in temperature of the more intense peak (510 °C). Sampling of the evolved gas phase for TG−GC−MS analysis was performed at the same temperatures detected for DTG peaks, as shown in Figure 2. The results concerning the TG−GC−MS gas-phase analyses are summarized in Table 1 which presents also the semiquantitative determination of the more representative detected species. At 272 °C, the evolved gas phase is mainly composed of CH_4 with lower amounts of Cy3, Pr^{n}OH, CO, and Cy4 and traces of EtOH. At 470 °C, the main species becomes Cy3, followed by Cy4, CO, and CH_4; small amounts of Si−Cl, M2, and a unidentified siloxane oligomer ($t_R = 91.1$) are also present.

Further information can be achieved analyzing the trend of suitable IC vs time (Figure 3) which allows the evolution of the different volatiles to be related to single or different phenomena taking place at different temperatures.

DZR20 Xerogel. Figure 1b presents the TG, DTG, and TIC patterns of DZR20 gel. The TG curve presents a weight loss characterized by two different steps in the 80−340 °C (10.0 wt %) and 340−800 °C (43.5 wt %) intervals. The DTG is characterized by two peaks at 275 and 481 °C with a small shoulder at 675 °C. The TIC shows two peaks at 300 and 485 °C, the latter being twice as intense as the former. Other effects are present as shoulders at 170, 560, and 720 °C. Sampling was carried out in correspondence with the maxima of the DTG curve. At 275 °C, the main evolution of Cy3 species is observed associated with methane, CO, and Pr^{n}OH with traces of EtOH and Cy4. At 482 °C, Cy3 and Cy4 are the more important evolved species with lower contents of CH_4, Si−Cl, and M2, and traces of TMS and the unindentified species at $t_R = 91.1$ (Table 1). From IC vs temperature diagrams, Cy3 (*m*/*z* 207) and Cy4 (*m*/*z* 281) species show a trend analogous to that of the TIC curve. A similar behavior is detected for M2 (*m*/*z* 147, 66) which presents the second most intense peak slightly shifted to higher temperature (535 °C). A wide band at 550 °C is due to Si−Cl; Pr^{n}OH evolution is centered at 190 °C while water shows two superposed peaks: a broad one centered at 135 °C and a sharp effect at 245 °C. Methane presents a first peak at 305 °C followed by two overlapped bands at 580 and 670 °C.

DZR10 Xerogel. The TG curve is characterized by two main steps in the 60−340 °C interval with 8.6% intensity and 340−800 °C with 66.4% intensity. In the DTG curve two small effects are present at 150 and 280 °C, followed by the main peak at 520 °C. The TIC trend is characterized by a peak at 280 °C with a small shoulder at 180 °C followed by a more intense peak centered at 505 °C (Figure 1a).

In the TG−GC−MS analysis two samplings were performed at 275 and 495 °C, respectively. The first sampling, at 275 °C, shows the main evolution of Cy3 species associated with methane and an unidentified siloxane species ($t_R = 213.9$) with minor amounts of Cy4, Pr^{n}OH, and CO. At 495 °C, the gas phase is composed mainly of Cy3 followed by Cy4, with the minor presence of Si−Cl, CH_4, CO and the unindentified species at $t_R = 91.1$ (Table 1). From the TG-MS analysis, the behavior of Cy3 (*m*/*z* 207), Cy4 (*m*/*z* 281), and M2 (*m*/*z* 147 and 66) siloxane species is the same as that observed for DZR20. The evolution of Si−Cl (*m*/*z* 93) presents a maximum at 510 °C. The Pr^{n}OH evolution shows a peak at 190 °C while water is found at 250 °C. A sharp band at 280 °C, followed by a more intense peak at 595 °C with a shoulder at 690 °C, is detected for the CH_4 evolution.

DZR50 Xerogel. The TG curve of DZR50 (Figure 1d) shows a continuous weight loss up to 800 °C. Two main steps can be evidenced: an initial weight loss from 60 to 360 °C (21.8 wt %) and a second one in the 360−800 °C interval (10.0 wt %). The DTG behavior of DZR50 is appreciably different from the systems presented above, showing two overlapped strong peaks at 130 and 243 °C, followed by an asymmetric broad band from 360 to 800 °C centered at 671 °C. The first

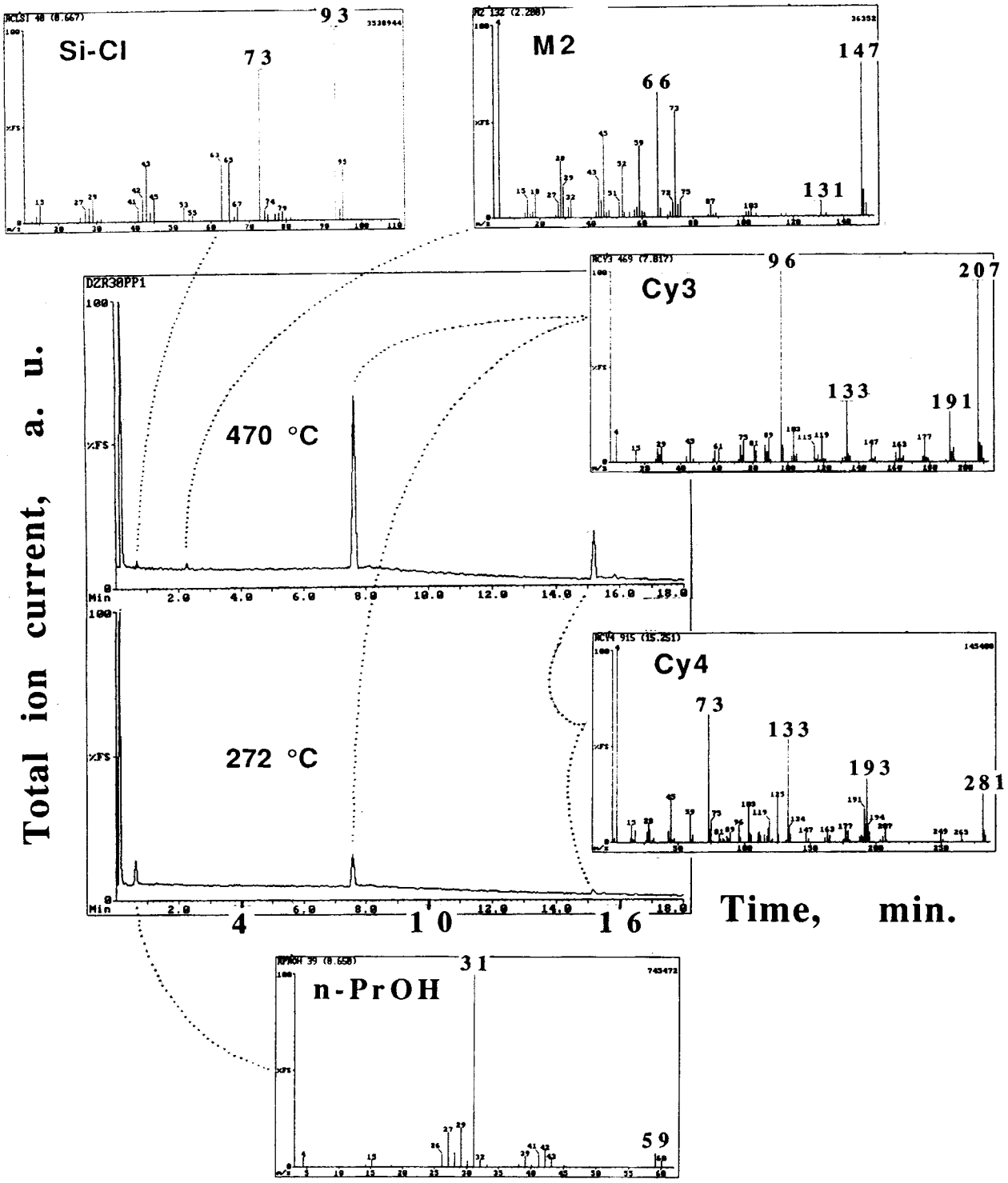

Figure 2. TG−GC−MS analysis of the gas phase evolved during DZR30 pyrolysis. Sampling was performed at the temperatures relating to DTG peaks shown in Figure 1C.

two intense peaks in the TIC curve appear overlapped and centered at 200 and 260 °C, showing an inversion in relative intensity with respect to the DTG pattern. At higher temperatures, three superimposed peaks are well-defined with maxima at 424, 497, and 661 °C, respectively; their relative intensity ratio is different from the DTG peaks. Four samplings were carried out (Figure 4). The results, reported in Table 1, point out that methane is always present as the predominant species, being the only one detected at 663 °C. Moreover, the cyclic oligomers, constituting the predominant evolved species in DZR*x* with $x \leq 30$, are not revealed throughout the whole pyrolysis process. At 244 °C, in addition to CH_4, Pr^{n}OH, lower amounts of CH_4, CO, and CO_2 and traces of EtOH and acetone are found. Besides methane, at 424 °C, the gas phase is composed of lower amounts of CO and propene; furthermore, at 497 °C, CO, M2, TMS, CO_2, and propene are easily detectable. For this sample, Figure 5 reports the evolution of the more representative species. It should be said that the band at 235 °C in the propene (*m*/*z* 42) IC curve is probably generated by the contribution of the Pr^{n}OH ionic fragmentation.

Table 1. TG−GC−MS Results Obtained on DZR*x* Gels

sample	weight loss (temp, °C)	weight loss intensity, %	TG−GC−MS sampling temp,°C	chemical species (%)[a]
DZR10	I (60−340)	8.6	275	CH_4 (11), PrOH (3), Cy3 (33), Cy4 (6), X1[b] (15)
	II (340−800)	66.4	495	CH_4 (1), Si−Cl (2), M2 (1), Cy3 (78), Cy4 (13), X2[b] (1)
DZR20	I (80−340)	10	275	CH_4 (14), PrOH (2), Cy3 (39), Cy4 (<1)
	II (340−800)	43.5	482	CH_4 (3), Si−Cl (1), M2 (1), Cy3 (72), Cy4 (14), X2[b] (<1)
DZR30	I (60−360)	13.4	272	CH_4 (45), PrOH (7), Cy3 (17), Cy4 (2)
	II (360−620)	20.8	470	CH_4 (4), Si−Cl (1), M2 (1), Cy3 (47), Cy4 (11), X2[b] (1)
	III (620−800)	3.9		
DZR50	I (60−360)	21.8	244	CH_4 (9), PrOH (5)
	II (360 → ...)		424	CH_4 (29), propene (10)
	III (... → ...)		497	CH_4 (26), propene (1), TMS (2), M2 (12)
	IV (... → 800)	10.0	663	CH_4 (70)

[a] Semiquantitative analysis calculated from the percentage of the normalized chromatographic peak area. [b] Unidentified siloxane species with >3 silicon atoms.

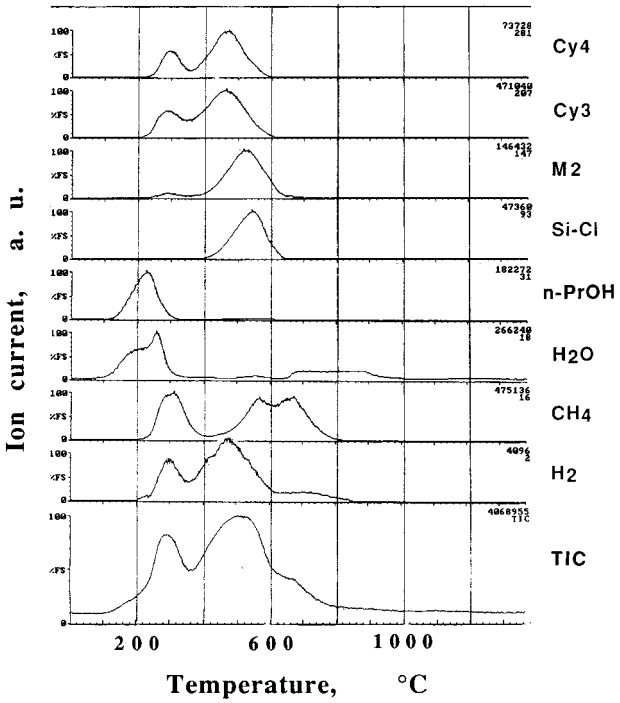

Figure 3. IC vs temperature diagrams for different gaseous species evolved during the pyrolysis of DZR30.

FTIR Study. Figure 6 presents the FTIR spectral evolution vs pyrolysis temperature for DZR10 (Figure 6a) and DZR50 (Figure 6b). The FTIR spectrum of the DZR10 xerogel is characterized by the strong absorptions due to the Si−O vibrations (νSi−O = 1017 and 1096 cm^{-1}) in typical D units.[12,21] At 1263 cm^{-1}, the sharp peak due to Si−CH_3 bond stretching is found. The sharp peak at 798 cm^{-1} is attributed to the Si−C stretching while the absorption at 865 cm^{-1} is due to the Si−CH_3 deformation.[21] At higher frequencies, the asymmetric and symmetric stretchings of methyl C−H bonds are found at 2965 and 2906 cm^{-1}, respectively. The broad and weak band centered at 3425 cm^{-1} is due to O−H stretching of adsorbed water. At 400 °C, the FTIR spectrum of DZR10 appears unchanged showing a slightly increased amount of surface adsorbed water. A different pattern is observed at 600 °C that shows clear changes in the bands due to Si−O stretchings, which now appear as a single broad band centered at 1030 cm^{-1}. A slight frequency shift is observed for the Si−CH_3 stretching (1266 cm^{-1}) vibration whose intensity is strongly reduced. The same decrease is observed for the Si−C stretching and Si−CH_3 deformation peaks. A new broad band appears at 466 cm^{-1} attributed to Si−O−Si deformation, whose position indicates the change of the overall condensation degree of the Si units.[12] A further increase of water presence is observed. At 800 °C, signals related to Si−C and C−H bonds disappear. A more symmetric but still broad Si−O band is observed together with a more defined Si−O−Si band at 467 cm^{-1}. The increase of adsorbed water appears more evident at this temperature. The trend of FTIR spectra vs temperature described for DZR10 is representative also of the pyrolysis behavior of DZR20; DZR30 behaves in the same way, a starting transformation of the Si−O related absorptions being observable already at 400 °C. Figure 6b presents the evolution of the DZR50 FTIR spectra versus temperature. The DZR50 xerogel spectrum shows features related to a structural arrangement different from that described for the previous systems. An asymmetric band centered at 3420 cm^{-1} and a shoulder at 3665 cm^{-1} are due to the O−H stretching in adsorbed water and silanols,[21] respectively. Peaks related to the Si−CH_3 groups are present at 1260 (νSi−CH_3), 861 (ρSi−CH_3), and 798 (νSi−C) cm^{-1}, showing a slight shift toward lower frequencies for the Si−CH_3 absorptions. A complex band generated by overlapping of at least four peaks at 1044, 1018, 980, and 933 cm^{-1} accounts for the Si−O and Si−OH absorptions, where vibration at 1018 cm^{-1} could be partially attributed to the Si−O−Zr bonds[22] and the peak at 933 cm^{-1} is indicative of the Si−OH bonds. The well-defined peak at 449 cm^{-1} is probably due to the superposition of the Si−O−Si deformation mode and Zr−O stretching, according to the signal at 460 cm^{-1} we have found in zirconium oxopolymers precipitated from an aqueous solution of $Zr(OPr^n)_4$.[23] A lower thermal stability is observed for DZR50 since, at 400 °C, the Si−CH_3 absorption peaks decrease in intensity and a noteworthy change is observed in the Si−O absorption pattern associated with the high-frequency shift of the Si−OH stretching (941 cm^{-1}). Increasing the temperature results in the progressive decrease of the Si−CH_3 absorptions and the disappearance of the Si−OH vibrations. At low frequencies, the

(21) Launer, P. J. *Silicon Compounds*; Petrarch Systems Inc.: Karlsruhe, Germany, 1987; p 77.

(22) Abe, Y; Sugimoto, N.; Nagao, Y.; Misono, T. *J. Non-Cryst. Solids* **1989**, *108*, 150.

(23) Rigo, L., Thesis, University of Trento, 1997.

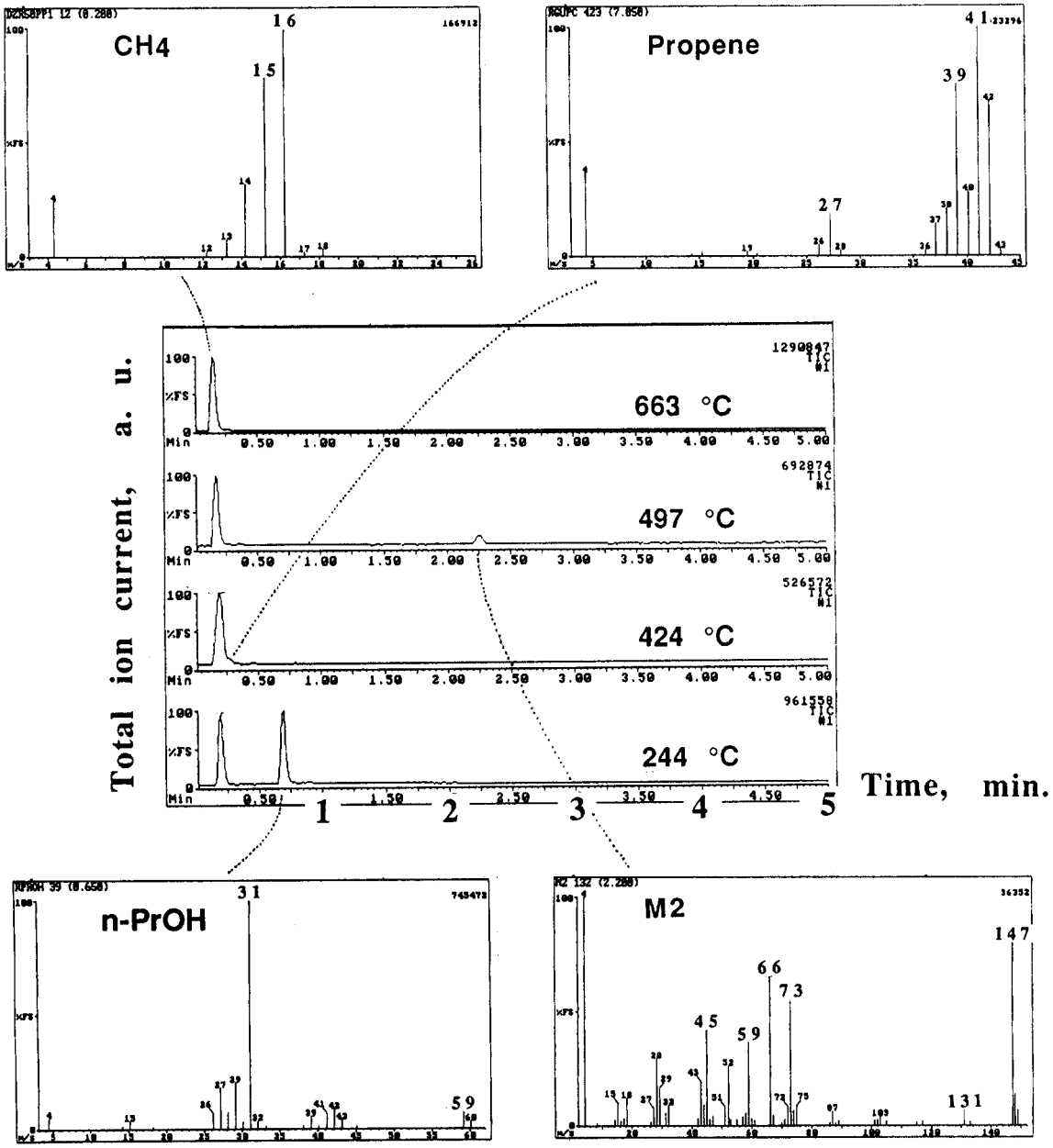

Figure 4. TG−GC−MS analysis of the gas phase drawn at the temperatures corresponding to DTG peaks shown in Figure 1D for DZR50 sample.

peak at 454 cm^{-1} presents a shoulder at 528 cm^{-1}, indicating an increasing order in the ZrO_2-based phase.[22,24]

Surface Area Determination. Figure 7a reports the evolution of the DZR30 specific surface area against pyrolysis temperature as an example of the pyrolysis behavior of the DZR*x* gels. At low temperature, all samples display a very low surface area which increases, reaching the greatest value at 600 °C. Further heating beyond 600 °C leads to a progressive collapse of the porous structure. The comparison between the DZR*x* samples at 600 and 800 °C is shown in Figure 7b. The specific surface area (SSA) increases with percent DEDMS at both temperatures, reaching for DZR10 630 and 440 $m^2\ g^{-1}$ at 600 and 800 °C, respectively. From the N_2 desorption isotherm of DZR10 at 800 °C using the Kelvin equation, a narrow pore size distribution is obtained with a mean pore radius of 20 Å.

(24) Miranda-Salvado, I. M.; Serna, C. J.; Fernandez Navarro, J. M. *J. Non-Cryst. Solids* **1988**, *100*, 330.

Discussion

Hybrid DZR*x* gels can be easily obtained starting from mixtures of DEDMS and $Zr(OPr^n)_4$. They appear transparent and homogeneous with a more intense yellow color as the Zr content increases. Moreover, their mechanical behavior is strictly related to the composition, changing from compliant to brittle materials with increasing Zr content. These hybrid xerogels have been previously described, using spectroscopic techniques,[5,7,10] as nanocomposites constituted of poly(dimethylsiloxane) chains acting as bridges between zirconium oxide based particles. Moreover, ^{29}Si MAS and CP-MAS NMR spectra of DZR*x* have pointed out the presence of cyclic oligomers entrapped in the hybrid matrix together with constrained siloxane units, probably due to silicon units

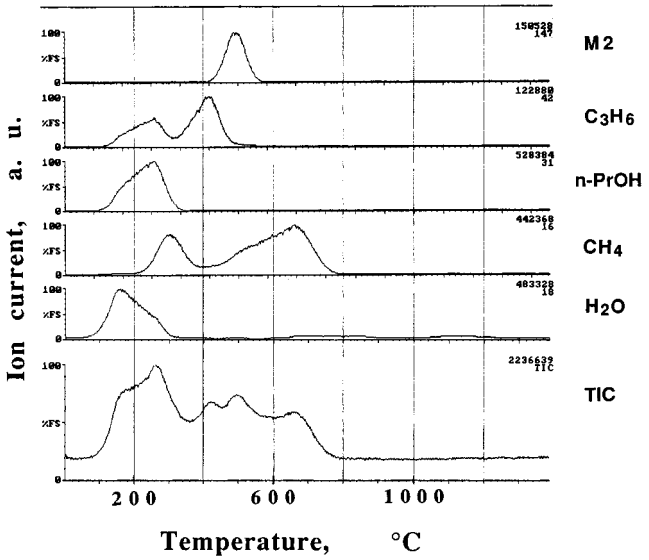

Figure 5. IC vs firing temperature diagrams of different evolved species for DZR50.

close to the zirconia phase.[7] The amount of D units in a constrained environment was around 10% in DZR10 and was shown to increase with increasing Zr content.[10] Actually, unpublished Zr K-edge EXAFS results on DZR20 sample suggest the preservation of few Si−O−Zr bonds in the xerogel state; thus, the $k^3\chi(k)$ Fourier transformed curve is better simulated by taking into account the Zr−O distances together with the silicon atoms as possible second nearest neighbors. Recently, Sanchez et al.[25] have described DZR*x* xerogels, produced following our synthesis procedure, as nanocomposites made of hydrophobic poly(dimethylsiloxane) chains covalently linked to hydrophilic domains made of zirconium oxopolymers. Their results indicated that terminal groups are present on the zirconium oxopolymers and the size of the ZrO_2-based domains is about a few nanometers, as indicated by SAXS. Moreover, using ^{17}O MAS NMR, they were able to identify, in the DZR20 xerogel, OZr_3, OZr_4, and OSi_2 species due to homocondensation together with a broad component attributed to Si−O−Zr bonds.

The general behavior toward pyrolysis of DZR*x* xerogels is well-represented by the TG, DTG, and TIC trend vs temperature, where a similar trend is observable for Zr% ≤ 30, while a very different profile is exhibited by DZR50. The weight loss steps appear strongly related to the chemical composition of the DZR*x* xerogels; an increase in the first weight loss intensity and a decrease of the second one is observed with increasing Zr content.

During the pyrolysis process of the DZR*x* samples, the methane evolution observable along the whole thermal process, and surprisingly even at temperature as low as 250 °C, is quite remarkable. Disregarding the sample composition, the methane evolution is described by different phenomena at various temperatures (Figure 3), suggesting different condensation mechanisms. At low temperature, methane loss increases with increasing Zr%, as revealed by the semiquantitative calculations performed on GC−MS analyses (Table 1). The

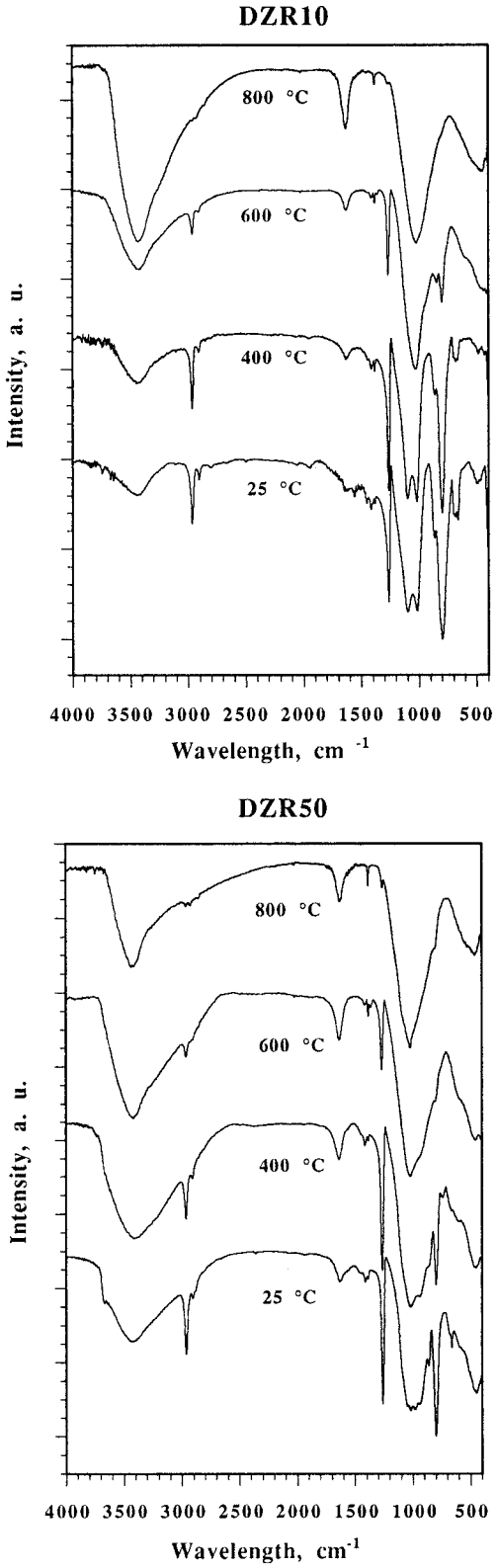

Figure 6. FTIR spectra evolution vs pyrolysis temperature for (top) DZR10 and (bottom) DZR50 samples.

evolution of CH_4 should involve Si−CH_3 bond cleavage which is known to take place above 600 °C in polysiloxane-derived materials.[15,26] However, Peeters et al. have recently reported the influence of a heteroatom like aluminum in decreasing the thermal stability of the

(25) Schaudel, B.; Guermeur, C.; Sanchez, C.; Nakatani, K.; Delaire, J. A. *J. Mater. Chem.* **1997**, *7(1)*, 61.

(26) Belot, V.; Corriu, R. J. P., Leclercq, D.; Mutin, P. H.; Vioux, A. *J. Polymer Sci. A* **1992**, *30*, 613.

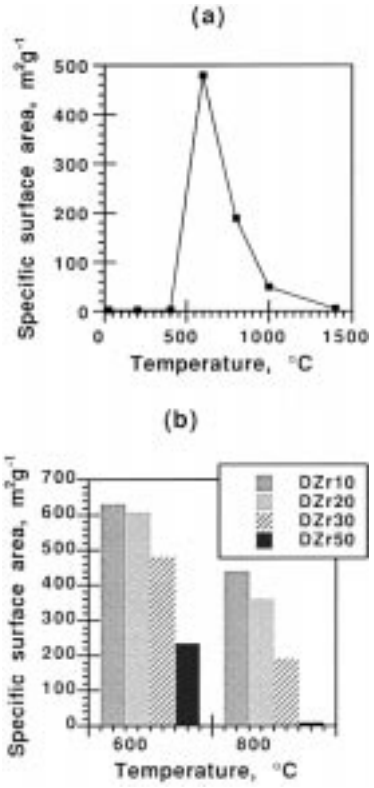

Figure 7. Evolution of DZR30 specific surface area against pyrolysis temperature (a) and comparison between specific surface area presented by DZR*x* samples at 600 and 800 °C, respectively (b).

Si−C bond in trifunctional siloxane-derived materials.[27] In our case, the role of the transition metal should be invoked to account for the low-temperature Si−C bond breaking, as suggested by the reaction

$$\equiv Si-CH_3 + H-O-Zr\equiv \rightarrow \equiv Si-O-Zr\equiv + CH_4 \quad (1)$$

which involves the transformation of D into T units due to the reaction between the terminal OH groups of the zirconium oxopolymers and D units either present at the interface between hydrophobic/hydrophilic domains or belonging to mobile chains at a suitable distance from the ZrO_2-based phase. According to reaction 1, a slight decrease of the Si−CH_3 and Si−C stretching intensities is observed in the IR spectra for samples heated to 400 °C, with respect to the Si−O absorption peaks. This behavior is more evident as the Zr% increases, as well as the modification of the Si−O vibration pattern. Moreover, the higher frequency shift of the Si−CH_3 stretching, probably due to a more constrained structure, confirms the proposed conversion of D units into T units.[21]

In the first weight loss, cyclic siloxane oligomers are the prevailing evolved species according to previous results on silicones and siloxane-derived hybrid gels.[15,26,28] In these studies, the release of cycles is attributed mainly to Si−O/Si−O redistribution reactions, ensuring the maintenance of the silicon functionality.[26] The evolution of cycles during the pyrolysis of DZR*x* samples is always indicated in TG−MS analyses by two bands centered around 270 and 500 °C, the former band being always the less intense. Taking into account the observed ability of the transition metal atom to induce bond cleavage, a more probable release of chain fragments such as the cyclic oligomers should be expected in samples richer in ZrO_2. On the contrary, the amount of released cyclic siloxanes decreases during the first weight loss with increasing Zr content. For these reasons, we believe that the cyclic species evolved in the first weight loss step are mainly those entrapped in the gel network during the hydrolysis−condensation process. The probability to produce long siloxane chains or cyclic oligomers during the gelling process of DEDMS depends on the possibility to form intermediates presenting bridging oxygens between silicon and zirconium atoms.[7,8] If the amount of zirconium atoms available to condense with the Si−OH groups is low, the condensation process should lead to the formation of siloxane chains, generating the gel network together with a substantial amount of cyclic oligomers which will remain entrapped in the low polarity silicon-rich phase. According to these arguments and the experimental evidence in the DZR10 ^{29}Si MAS NMR spectrum of a signal at −19.3 ppm attributed to the presence of tetrameric cycles,[7] the release of cycles by stripping from the gel network is favored in the case of the DZR10 sample. The low amount of available zirconium atoms during the condensation can also produce, for DZR10, the formation of polysiloxanes with higher molecular weight than Cy3 and Cy4, as deduced from the detection of species with high retention time in GC−MS analyses, although their MS spectra do not allow a definitive attribution. The loss of volatiles entrapped in the network cannot produce any modification of the gel structure; in fact, the comparison of the FTIR spectra of DZR10 at room temperature and 400 °C seems to confirm this hypothesis. On the other hand, the change in the Si−O vibrations from room temperature to 400 °C observed for higher Zr contents and particularly in the case of DZR50 could be mainly attributed to the cross-linking effects due to reaction 1.

All samples show the evolution of water and PrOH localized at the beginning of the first peak present in the TIC curve (Figure 1). This fact is more evident by observing the trend of *m*/*z* 18 and 31 signals in Figure 3. This contribution increases in intensity as the Zr% increases, i.e., as the network becomes more and more hydrophilic. Since water and PrOH released during this stage are the byproducts of the hydrolysis condensation process, they are better retained in a polar matrix. In agreement with this hypothesis, the FTIR spectra of the DZR*x* xerogels show an increase in intensity of OH stretching with increasing Zr%. The trend of *m*/*z* 18 vs temperature shows a broad band with an overlapped peak centered at 260 °C (Figure 3). The first effect is probably due to water physically entrapped in the gel network, whereas the second one could be attributed to the condensation reaction of residual OH groups taking place in the hydrophilic Zr-rich domains (reaction 2).

$$\equiv Zr-O-H + H-O-Zr\equiv \rightarrow \equiv Zr-O-Zr\equiv + H_2O \quad (2)$$

The increase in PrOH evolution is more important with increasing Zr content. This phenomenon could be

(27) Peeters, M. P. J.; Kentgens, A. P. M.; Snijkers-Hendrickx, I. J. M. *Mater. Res. Soc. Symp. Proc.* **1996**, *435*, 415.
(28) Scott, D. W. *J. Am. Chem. Soc.* **1946**, *68*, 356.

justified by the greater amount of residual Zr−OPr^n groups due to the increasing substoichiometry in the water/alkoxide ratio used in gel preparation. Actually, the FTIR spectra (Figure 6) of the DZR10 and DZR50 xerogels show C−H absorption signals which can be best attributed to the CH_3 groups. The ^{1}H MAS NMR spectrum of DZR10 reveals a high degree of conversion of the alkoxy groups since it is dominated by the sharp Si−CH_3 signal;[7] the situation is more ambiguous for DZR50, where the broadening of the main Si−CH_3 signal and the spinning sidebands only allow one to suppose the presence of other signals.[7] However, we believe that the presence of CH_2 radicals in OPr^n groups cannot be neglected. These residual OPr groups may undergo a condensation reaction, consuming available Zr−OH groups according to reaction 3:

$$\equiv Zr-OPr + H-O-Zr\equiv \rightarrow \equiv Zr-O-Zr\equiv + PrOH \quad (3)$$

In the absence of available OH groups, the propoxide groups are later consumed at higher temperatures by elimination of propene (reaction 4), as observed in the case of DZR50, where this effect generates the second peak at 424 °C in the TIC curve (Figure 1d).

$$\equiv Zr-O-(CH_2)_2-CH_3 \rightarrow \equiv Zr-OH + CH_2{=}CH-CH_3 \quad (4)$$

The second weight loss step, starting from ≈350 °C, is the product of rearrangement reactions and polymer-to-ceramic transformation. The lower temperature of this stage in DZR*x* samples in comparison with the analogous processes during firing of DEDMS/tetraethoxysilane (TEOS) derived gels is noteworthy, where the evolution of silicon oligomers was detected mainly around 600 °C and hydrocarbons were released only above 650 °C.[15] At this stage, the Cy3 and Cy4 evolution is related to redistribution reactions occurring along the siloxane chains. This rearrangement can involve both Si−O/Si−O and Si−O/Si−C bond exchanges.[15,26] In the first case, the silicon functionality is maintained whereas in the second case the redistribution reactions lead to the production of different silicon units and a more cross-linked network. Si−O/Si−O exchange can involve silicon atoms along a single chain according to Scheme 1, with the consequent cycle evolution and binding of residual chain fragments. This phenomenon is expected in the case of longer and compressed helicoidal siloxane chains, which are more probable for DZR10 than DZR30.

The second mechanism for the release of cyclic oligomers involves the Si−O/Si−C bond exchange invoked when the chain envelope does not allow the hooking of the two fragments of the broken chain. In this case the support of a silicon atom available at a suitable distance on a second chain is required, leading to a modification of the average network functionality as shown in Scheme 2a,b.

The linear chain fragment evolution should involve a double exchange between Si−O and Si−C through the mediation of two silicon units present on nearby chains, as shown in Scheme 3 in the case of the M2 evolution.

Scheme 1

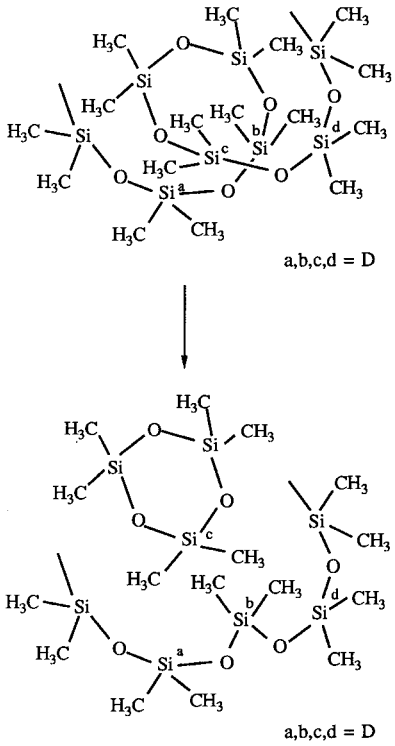

However, this last effect is statistically less probable and requires the transformation of two D units into M and T units.

The DZR*x* xerogels were previously described as two phase systems, constituted of siloxane chains and oxide particles. On the other hand, we note the transformation from elastic to brittle materials observed with the increase of ZrO_2 content, related to a more constrained polymeric phase. In our opinion this evidence could indicate that, varying the Zr%, chains of different length link the zirconia-based particles, as proposed in Figure 8. Thus, the DZR10 matrix can be described by long, rolled up, and spaced out siloxane chains, whereas the close proximity between Si sites and ZrO_2 particles in DZR50 gives rise to short, crowded, and more stretched siloxane units. On the basis of this structural interpretation, a more important evolution of cycles by Si−O/Si−X (X = O, C) exchange reactions is expected for low Zr contents. Moreover, the reactions given in Scheme 3 will become more probable in the DZR50 sample, where M2 evolution reaches a 12% intensity. As a matter of fact, decreasing the chain length results in a more probable release of volatiles generated by the Si−C cleavage with respect to those produced by the Si−O bond breaking. This observation agrees with the presence of the monomeric silicon unit, TMS, observed only during the DZR50 pyrolysis.

The Si−C bond cleavage is followed by methane evolution, which is indicative of the polymer to ceramic transformation. The introduction of carbon atoms into an oxycarbide network can be ascribed to the following reactions:[15]

$$2(\equiv Si-CH_3) \rightarrow \equiv Si-CH_2-Si\equiv + CH_4 \quad (5)$$

$$\equiv Si-CH_2-Si\equiv + \equiv Si-CH_3 \rightarrow (\equiv Si)_3-CH + CH_4 \quad (6)$$

Scheme 2

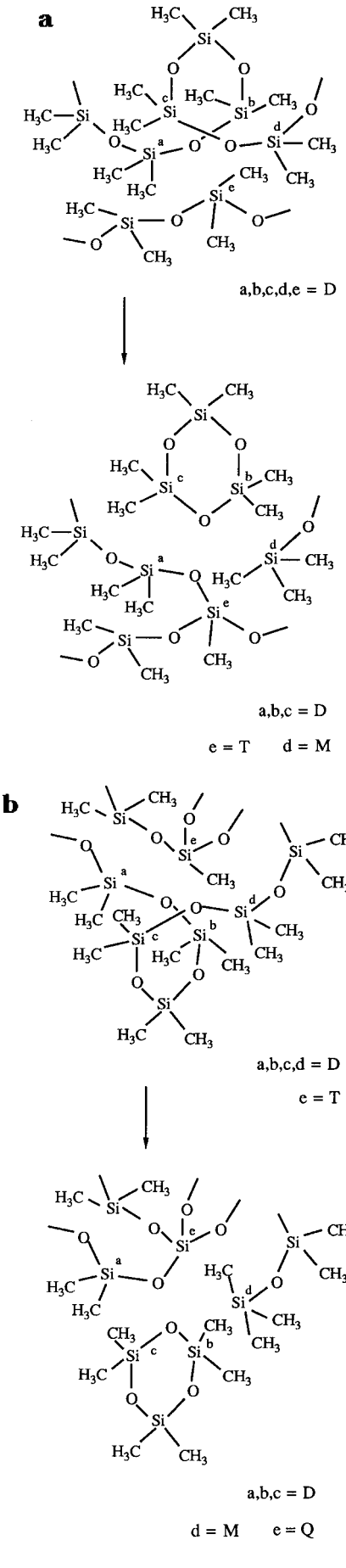

Scheme 3

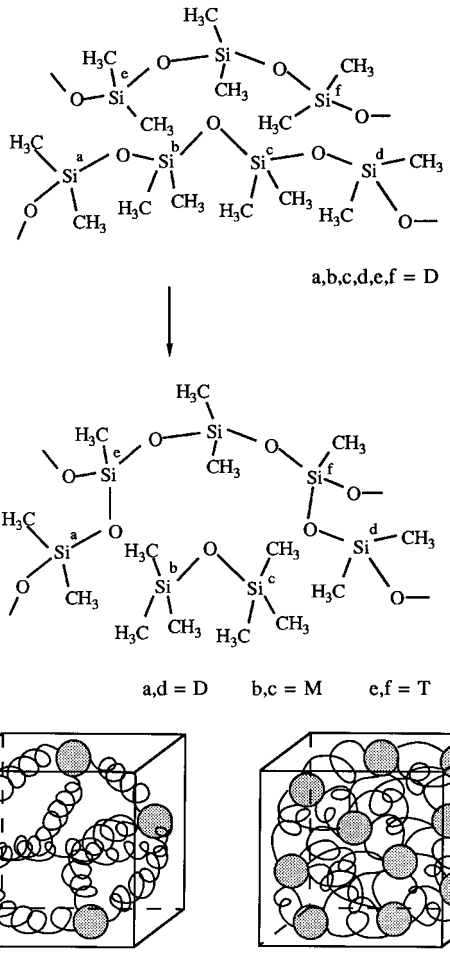

Figure 8. Different structural arrangements between poly(dimethylsiloxane) chains and zirconia particles in function of the chemical composition for DZR*x* gels.

As expected, CH_4 evolution at high temperature is proportional to the Zr content as a consequence of the low chain length and the lower dissociation energy required for Si−C cleavage with respect to the Si−O bond. The network modification due to reactions 5 and 6 is clearly observed in the FTIR spectra at 600 °C, where a decrease of the Si−CH_3 and Si−C stretchings is observed; the Si−CH_3 bond consumption appears almost complete at 800 °C. A parallel modification is observed for the Si−O−Si band, which shifts toward higher frequencies and becomes broader, with the partial superposition of signals due to an ordered ZrO_2 phase in the case of DZR50, in agreement with TEM evidence of the starting crystallization of t-ZrO_2 at 800 °C.[29] The Si−O absorption peak at 800 °C is present at lower frequency than the signal expected for a pure silica phase, probably indicating the formation of an oxycarbide network. Preliminary ^{29}Si MAS NMR results on DZR*x* samples at 1000 °C confirm the presence of a SiC_xO_{4-x} phase which produces at 1400 °C a mixture of SiO_2 and α- and β-SiC.[29] The detailed study of the structural transformation at high temperature, including the morphology and the crystallization of the

(29) Dirè, S.; Ceccato, R.; Gialanella, S.; Babonneau, F. Unpublished results.

DZR*x* xerogels, will be published elsewhere; however, considering these first results, it seems that the DZR*x* pyrolysis pathway should be different from that occurring in the DEDMS/Ti(OPr^i)4 derived gels, whose polymer-to-ceramic conversion is currently under investigation. As a matter of fact, the pyrolysis of DTi30 produces, above 800 °C, a mixture of silica and titanium carbide as a consequence of the reactions between Si−C and Ti−O bonds to form Si−O and Ti−C bonds.[18]

The FTIR spectra at 600 and 800 °C show an increased presence of adsorbed water, according to the development at these temperatures of a high surface area as a consequence of the relevant chain rearrangements with the evolution of large quantity of volatiles. The case of the DZR10 sample is noteworthy where, starting from an almost dense structure (SSA < 10 m^2 g^{-1}), the SSA reaches 630 m^2 g^{-1} at 600 °C, in agreement with the more important second weight loss in the TG curve.

According to the results reported by Babonneau et al.,[15] the water evolution observed in our samples in the 650−900 °C interval (Figure 3) could be related to the radical breaking of the siloxane bonds, which yields at this temperature reactive Si−OH groups:

$$\equiv Si-O-Si\equiv + \equiv C-H \rightarrow \equiv Si-OH + \equiv C-Si\equiv \quad (7)$$

$$2(\equiv Si-OH) \rightarrow \equiv Si-O-Si\equiv + H_2O \quad (8)$$

Despite the low quantity, the evolution of $ClSiMe_3$ has been clearly detected during the pyrolysis of DZR10−30 samples. Its presence was unexpected since no presence of Si−Cl bonds was observed in the starting precursor. In our opinion, the likelihood of observing gas-phase reactions between evolved HCl and siloxane units to yield chlorosilane species is quite low, due to the dilution of the evolved species by the flowing carrier gas. Moreover, the HCl required for gas-phase reaction should evolve at temperatures lower than the one observed for the Si−Cl release. Consequently, it could be proposed that the formation of Si−Cl bonds occurs during the early stages of the gelling process, by HCl hydrolysis of siloxane units, as indicated by reaction 9:

$$\equiv Si-O-Si\equiv + H-Cl \rightarrow \equiv Si-OH + Cl-Si\equiv \quad (9)$$

The Si−Cl moiety survival inside the network is possible only in the absence of water which, if present, readily converts Si−Cl into Si−OH bonds. Accordingly, Si−Cl species is evolved only during pyrolysis of samples richer in DEDMS, which show a more hydrophobic behavior, whereas the more hydrophilic DZR50 gel shows TMS release.

Conclusions

The study of the gas-phase evolved during the pyrolysis of poly(dimethylsiloxane)−zirconia hybrid gels has been performed by coupling TG, GC, and MS techniques. This approach allowed us to obtain some insight into the chemical reactions occurring between the zirconium and silicon precursors during gel formation. On the basis of the different species evolved during the pyrolysis process, a different arrangement between the zirconium oxopolymers and the silicon-derived counterpart has been proposed as a function of the DEDMS/ZR molar ratio.

Despite the progressive feature changes of the DZR*x* gels and the maintenance of a macroscopic homogeneity, a borderline behavior was observed for theDZR50 specimen. DZR*x* gels with *x* up to 30 show during pyrolysis the typical behavior of oxide-modified siloxane resins, whereas in DZR50 the thermal evolution is closer to the changes observed in oxide-based materials.

The role of the zirconium atom in decreasing the thermal stability of the DZR*x* gels in comparison with the siloxane−silica samples was pointed out as taking into account the low temperature required for siloxane oligomers and methane evolution due to Si−O and Si−C bond cleavage.

Acknowledgment. Dr. Florence Babonneau is greatly aknowledged for the useful discussion and criticism. MURST is acknowledged for financial support. The authors are grateful to Prof. Giovanni Carturan who introduced them to the study of sol−gel process.

CM9704140